Annales Geophysicae (2004) 22: 2463–2472
SRef-ID: 1432-0576/ag/2004-22-2463

Annales Geophysicae

Separating spatial and temporal variations in auroral electric and magnetic fields by Cluster multipoint measurements

T. Karlsson[1], **G. T. Marklund**[1], **S. Figueiredo**[1], **T. Johansson**[1], **and S. Buchert**[2]

[1]Department of Plasma Physics, Alfvén Laboratory, KTH, SE-100 44 Stockholm, Sweden
[2]Swedish Institute of Space Physics , Box 537, SE-751 21 Uppsala, Sweden

Received: 27 September 2003 – Revised: 5 February 2004 – Accepted: 25 February 2004 – Published: 14 July 2004

Part of Special Issue "Spatio-temporal analysis and multipoint measurements in space"

Abstract. Cluster multipoint measurements of the electric and magnetic fields from a crossing of auroral field lines at an altitude of 4 R_E are used to show that it is possible to resolve the ambiguity of temporal versus spatial variations in the fields. We show that the largest electric fields (of the order of 300 mV/m when mapped down to the ionosphere) are of a quasi-static nature, unipolar, associated with upward electron beams, stable on a time scale of at least half a minute, and located in two regions of downward current. We conclude that they are the high-altitude analogues of the intense return current/black auroral electric field structures observed at lower altitudes by Freja and FAST. In between these structures there are temporal fluctuations, which are shown to likely be downward travelling Alfvén waves. The periods of these waves are 20–40 s, which is not consistent with periods associated with either the Alfvénic ionospheric resonator, typical field line resonances or substorm onset related Pi2 oscillations. The multipoint measurements enable us to estimate a lower limit to the perpendicular wavelength of the Alfvén waves to be of the order of 120 km, which suggests that the perpendicular wavelength is similar to the dimension of the region between the two quasi-static structures. This might indicate that the Alfvén waves are ducted within a wave guide, where the quasi-static structures are associated with the gradients making up this waveguide.

Key words. Magnetospheric physics (auroral phenomena; electric fields; plasma waves and instabilities)

Correspondence to: T. Karlsson
(tkarlsson@plasma.kth.se)

1 Introduction

In trying to obtain unambiguous spatially and temporally high resolution measurements of electric fields, currents and particle properties associated with the aurora, one has so far run into a dilemma. There has been the choice of either rocket or satellite in situ measurements, which provide very high time resolutions but suffer from the inherent spatio-temporal ambiguity of one-dimensional measurements, or two-dimensional, multipoint remote sensing methods, such as radar and optical observations, which are able to discern between spatial and temporal variations but do not provide the high resolution.

The resolution of the dilemma is to use multi-point, high-resolution in situ measurements. Early efforts include using data from conjunctions between several satellites of different orbits (e.g. Jorgensen and Spence, 1997), or rocket multipoint measurements, such as that obtained from the Auroral Turbulence II flight (Lynch et al., 1999; Ivchenko et al., 1999). The only continuous source of such multi-point measurements is presently the four Cluster satellites, which have been in scientific operation since 2 February 2001. In a paper by Marklund et al. (2001), the first results from a Cluster crossing of an evolving divergent electric field structure were reported, with the satellites crossing over a time of the order of a few minutes, in a string of pearls configuration.

In this paper we will present electric and magnetic field measurements from a Southern Hemisphere Cluster crossing of auroral field lines, and show how these can be used to separate spatial and temporal variations in the fields. The temporal and spatial scales probed in this event are shorter than those of the event investigated by Marklund et al. (2001), since the satellite configuration is different. This will provide us with unique information of the temporal and spatial scales and other properties of auroral electric field structures at Cluster altitude (4–5 R_E). A companion paper (Johansson et al., 2004; hereafter known as "the companion paper") will address the longer time scale temporal evolution of quasi-static structures in this and other events, and their detailed properties.

Table 1. Results of cross correlation analysis.

	Interval 1 t = 200 – 300 s	Interval 2 t = 300 – 380 s	Interval 3 t = 380 – 440 s
	dB	dB	dB
dt_{12} (s)	7.25	0.75	8.5
dt_{13} (s)	11.75	-1.0	13.0
dt_{14} (s)	0.5	0.0	5.75
dt_{23} (s)	2.5	0.5	4.5
dt_{24} (s)	-6.25	0.75	-2.25
dt_{34} (s)	-10.5	0.5	-6.5
	E	E	E
dt_{12} (s)	6.75		10.25
dt_{13} (s)	8.25		16.25
dt_{14} (s)	5.5		9.5
dt_{23} (s)	1.0		3.75
dt_{24} (s)	-1.25		0.0
dt_{34} (s)	-2.25		-3.75

2 Event overview

We will utilize data from two of the instruments on the Cluster satellites; the Electric Field and Wave Instrument (EFW) (Gustafsson et al., 1997), and the Fluxgate Magnetometer (FGM) (Balogh et al., 1997). The Cluster satellites were launched on 16 July and 9 August 2000 as a replacement of the original Cluster satellites which were lost due to a failure of the original launch in 1996. The orbit is polar with an apogee of 18.7 R_E and a perigee of 3.0 R_E. All four Cluster satellites have a spin period of 4 s.

The data investigated in this paper are from a pass over the southern auroral region close to perigee on 19 May 2002. Large variations in the electric and magnetic field were observed, and we concentrate on 600 s of data, starting from 05:26 UT. Data from the Plasma Electron and Current Experiment (PEACE) (Johnstone et al., 1997), not shown here, show that the large fields are observed when the Cluster satellites are situated within the plasma sheet boundary layer (PSBL), rather close to its poleward edge. The corrected geomagnetic latitude of the footpoint of the satellites for the time interval studied ranges from approximately 70° to 68.5°, the magnetic local time is close to 20:00 MLT and the geocentric distance is close to 5.0 R_E for the whole interval. Figure 1 shows the satellite positions (schematically) during the time from which the measurements are taken. The preliminary Auroral Electrojet index (available from the Data Analysis Center for Geomagnetism and Space Magnetism, Kyoto University, http://swdcwww.kugi.kyoto-u.ac.jp) indicates that the measurements take place during the peak of the expansion phase of a small to medium sized substorm, rather extended in time, and commencing at around 03:30 UT.

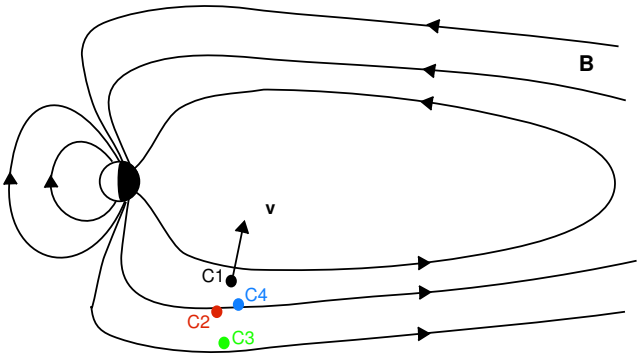

Fig. 1. Sketch of the position and configuration of the Cluster satellites at the around 05:26 UT on 19 May 2002.

3 Method and results

Figure 2 shows the residual magnetic field $d\boldsymbol{B}$ and the electric field $\boldsymbol{E}$, respectively, from Cluster 1–4. The colour coding is such that black corresponds to satellite 1, red to satellite 2, green to satellite 3, and blue to satellite 4. The residual magnetic field has been obtained by subtracting a running average with a window of 30 s from each field component. The Cluster satellites measure the electric field in the spin plane. The third component has been calculated by assuming that $\boldsymbol{E} \cdot \boldsymbol{B}$=0. This is a reasonable assumption, since at an altitude of 4 R_E, the Cluster satellites are most probably above the altitude where most of the acceleration takes place, which is usually at around 1–2 R_E in the upward current region (e.g. Weimer and Gurnett, 1993), and even lower in the downward current region (Marklund and Karlsson, 2001). All the electric and magnetic field components have then been smoothed by taking a running average with a window width of 3 s. This is to facilitate comparisons between all four satellites, since satellite 1 only provides the electric field with spin resolution, due to a failure of one of the probe pairs. In this paper we thus concentrate our attention on variations on time scales of 3–30 s in the satellite frame of reference. We use a coordinate system where x is parallel or anti-parallel to the local measured (total) magnetic field. Of these two directions, the one that is closest to $\mathbf{x}_{\mathrm{GSM}}$ is chosen to be the positive direction of x, i.e. our x coordinate is pointing in the general direction of the Sun. The z component is given by the projection of the Earth's dipole axis onto the plane perpendicular to x and positive in the approximately northward direction. The y direction completes the positively oriented system. Thus y corresponds roughly to a westward direction and z to a northward one, also in the Southern Hemisphere. Both figures show 600 s worth of data, starting from 19 May 2002, 05:26 UT.

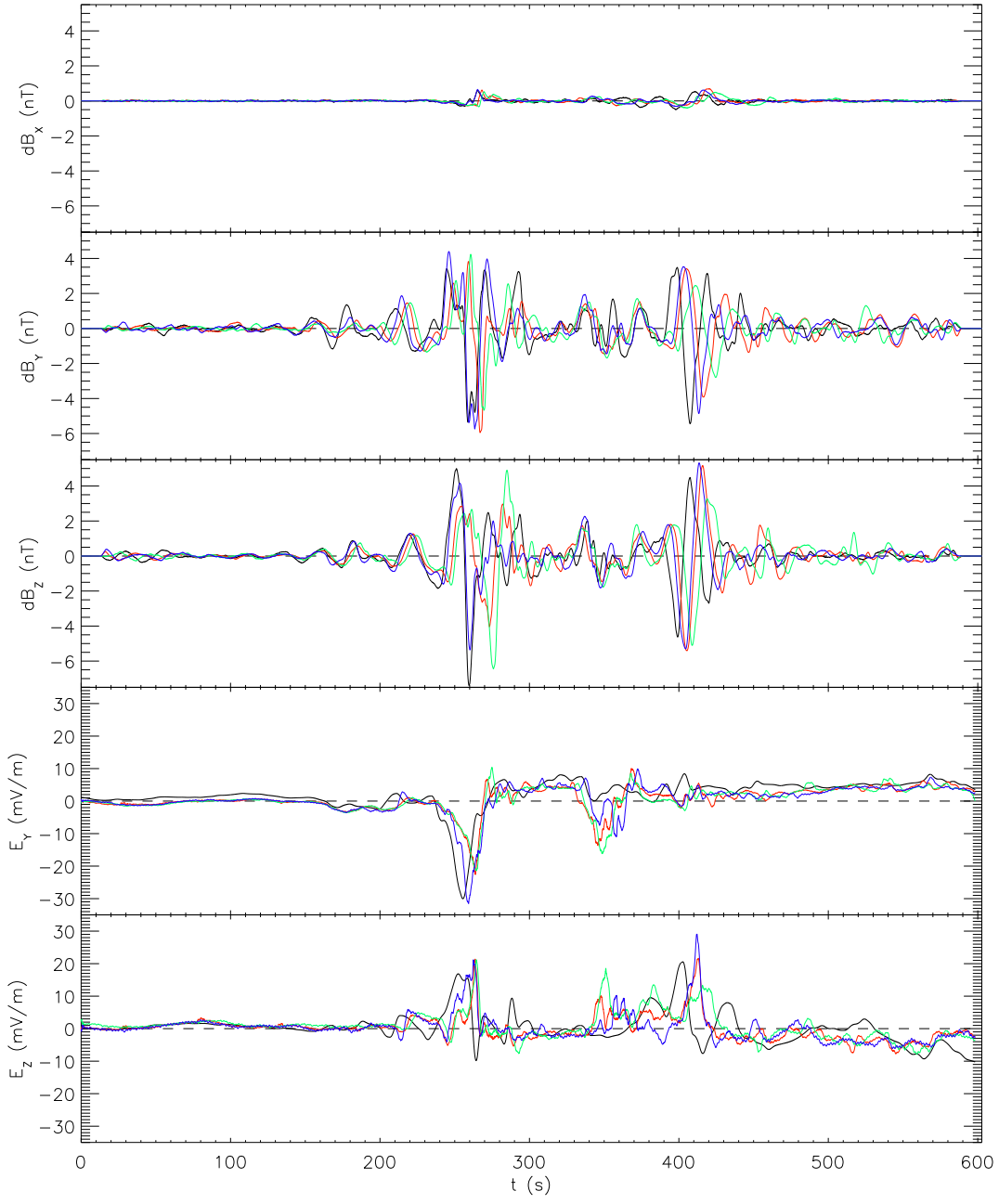

Fig. 2. Three components of the residual magnetic field $d\boldsymbol{B}$ and two components of the electric field $\boldsymbol{E}$ between 05:26 UT and 05:36 UT on 19 May 2002. The x-direction is anti-parallel to the ambient magnetic field, y and z are approximately to the geomagnetic west and north, respectively. E_x is identically zero due to the assumption that $\boldsymbol{E} \cdot \boldsymbol{B}$=0. In all panels data from all the four Cluster satellites are shown, with the following colour coding: Cluster 1 – black, Cluster 2 – red, Cluster 3 – green, Cluster 4 – blue.

From Fig. 2 we first note that dB_x is very small over the whole interval, and that there is thus very little compression in the magnetic field. We then note that the interval of appreciable magnetic field variations can be divided up into three intervals according to their spatio-temporal characteristics:

1. Between approximately 200 s and 300 s there are variations with a total amplitude of around 8 nT. These variations are easily recognizable between the satellites, and are observed almost simultaneously on satellites 1 and 4, whereas satellites 2 and 3 observe them 10–15 s later.

2. Between approximately 300 s and 380 s all satellites observe variations with an amplitude of around 3 nT. These variations appear not to be associated with any appreciable time shifts between the observations by the different satellites.

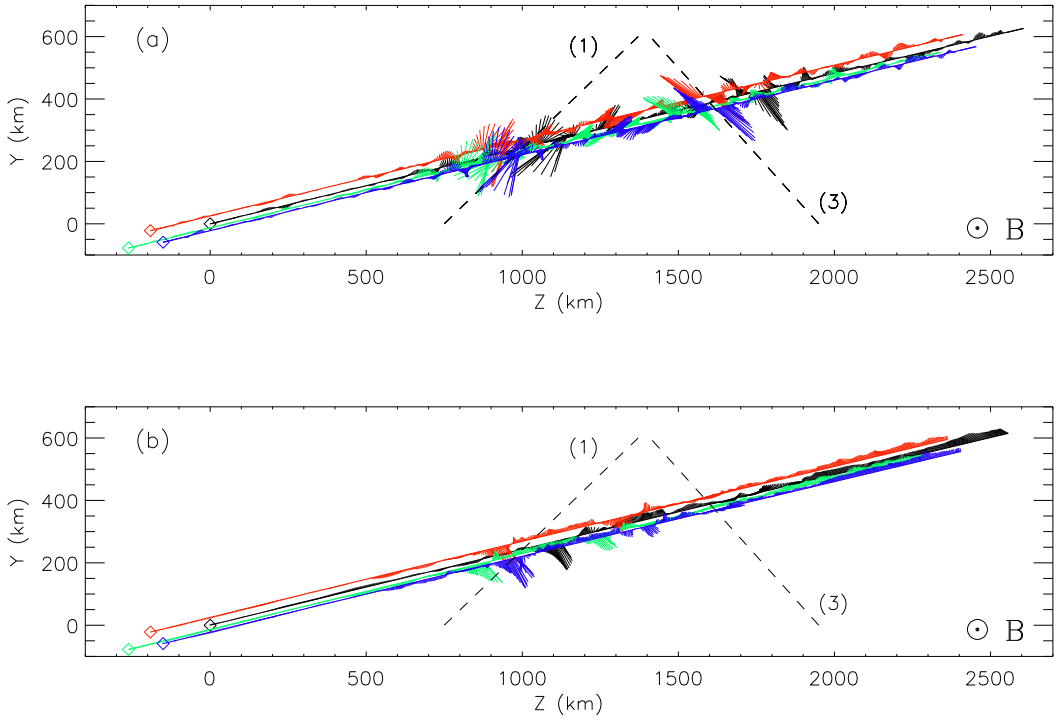

Fig. 3. Vector diagram of the residual magnetic field $d\boldsymbol{B}$ **(a)** and the electric field $\boldsymbol{E}$ **(b)** along the trajectories of the Cluster satellites, projected into a plane perpendicular to the magnetic field. As in Fig. 2, y and z are approximately to the geomagnetic west and north, respectively, and the colour coding is the same. Also indicated are the approximate orientations of the extended current sheets of regions (1) and (3), (see text).

3. Between approximately 380 s and 440 s there are again structures that are recognizable between the satellites, with a spread of time shifts up to around 20 s between satellites 1 and 3. The amplitude of these variations is slightly smaller than of those in interval (1).

The electric field exhibits a similar behaviour with comparable time shifts, although in intervals (1) and (3) they are clearly unipolar. The amplitudes of these unipolar electric field signatures are around 35 mV/m, and 30 mV/m in intervals (1) and (3), respectively. Mapped down to the ionospheric level this corresponds to approximately 350 and 300 mV/m. In interval (2) slightly weaker electric fields are observed, which are not unipolar. In this interval the electric field structures show a general similarity to each other, but do not have the same clear identity, recognizable between the different satellite crossings as the structures of intervals (1) and (3). We also draw attention to intervals of a constant electric field in an approximately westward direction between 280 s and 330 s, and about southwestward from around 450 s, remaining so directed for the rest of the measurement period.

In order to quantify the observations above regarding the time shifts between the satellite observations, we have performed a cross-correlation analysis, summarized in Table 1. In order to obtain as clear correlations as possible, we have proceeded in the following fashion: First, we have performed a minimum variance analysis (MVA) on $d\boldsymbol{B}$ and $\boldsymbol{E}$ for each satellite. We have then cross-correlated the dominant components of $d\boldsymbol{B}$ from each of the satellites with the corresponding measurement from all the other satellites, in a pair-wise fashion. For each of these pairs we have recorded the time shift that gives a maximum in the cross-correlation, for those combinations where a clear maximum was obtained. Thus, for example, the entries in the row marked dt_{12} indicate that for interval (1) the structures in $d\boldsymbol{B}$ are observed 7.75 s earlier on satellite 1 than on satellite 2. We have then done the same thing for $\boldsymbol{E}$. For some combinations of signals no clear maximum in the cross-correlation could be obtained; these correspond to blank entries in the table.

It can be seen that for intervals (1) and (3), the fluctuations in $\boldsymbol{E}$ and $d\boldsymbol{B}$ are consistently observed first by satellite 1, followed by satellites 4, 2, and 3, as schematically indicated at the bottom of Table 1. What changes between the intervals is the relative time shifts between the satellites. For interval (2) the time shifts in $d\boldsymbol{B}$ are all around zero, whereas there are no clear maxima in the correlations between the electric field signals. The fact that the time series of interval (2) are consistent with a zero time shift is a first indication that these structures are of a temporal nature.

In order to interpret these results we plot $d\boldsymbol{B}$ and $\boldsymbol{E}$ in Figs. 3a and b, respectively, as vector plots along the satellite trajectory in the y-z plane, i.e. in the plane perpendicular to

Table 2. Summary of results from cross correlation and minimum variance analysis.

	Cross-correlation analysis		Minimum variance analysis		$v_\perp$
	$\alpha(d\boldsymbol{B})$	$\alpha(\boldsymbol{E})$	$\alpha(d\boldsymbol{B})$	$\alpha(\boldsymbol{E})$	
Interval (1)	46°±8°	40°±13°	43°±5°	58°±3°	9.7±3.9 km/s
Interval (2)			45°±6°	55°±10°	
Interval (3)	−33°±20°	−42°±18°	−53°±8°	−2°±3°	17.9±4.2 km/s

the total magnetic field $\boldsymbol{B}$. (For these two plots, we fix the coordinate system by choosing x to lie along the measured magnetic field at t=300 s. The y and z directions are defined in the same way as earlier.) The position of each satellite corresponding to t=0 in Fig. 3 is marked by a diamond, and thus the mutual satellite separations in the plane perpendicular to $\boldsymbol{B}$ can be read off from the figure. The colour coding is the same as above.

In Fig. 3 both the magnetic field fluctuations associated with intervals (1) to (3), and the electric field fluctuations of interval (1) are easy to make out. (The electric field fluctuations of interval (3) are more difficult to make out in the figure, since they are directed almost along the satellite trajectory. We will discuss the direction of the electric field in this time interval later.) We note that none of the field structures line up in a consistent way in space. This means that none of them are pure spatial structures, stationary in the geomagnetic coordinate system used here. However, the fact that there are consistent time shifts enables us to interpret the observations in intervals (1) and (3) as quasi-stationary structures moving over the satellite, similar to Cluster observations of magnetopause crossings (Gustafsson et al., 2001; Pedersen et al., 2001; Dunlop et al., 2002). By assuming that the structures are elongated in a plane with no variations along the plane, at least over a length comparable to the satellite separations, we can determine the angle α of the plane and its velocity component $v_\perp$ perpendicular both to $\boldsymbol{B}$ and to the plane itself, which best reproduces the observed time shifts. By a trial and err method we obtain for interval (1), α=46°±8°, where α is the angle between the moving plane and the y axis, defined positive in the clockwise direction when looking in the direction opposite to $\boldsymbol{B}$, i.e. into the plane of the paper in Fig. 3a. The orientation of the plane is shown in Fig. 3a with a dashed line. For the velocity, we obtain 9.7±3.9 km/s, relative to the satellites. Subtracting the satellite velocity component perpendicular to $\boldsymbol{B}$ and to the moving plane gives us $v_\perp$=7.9 km/s±3.9 km/s. Mapped to the ionosphere, this corresponds to approximately 0.8 km/s. We then proceed in a similar way for interval (3). The results for both intervals are summarized in the left part of Table 2, where we give the results using both the time shifts in $d\boldsymbol{B}$ and $\boldsymbol{E}$. In order to validate this procedure we have also performed the cross correlation directly on both components of $d\boldsymbol{B}$ and $\boldsymbol{E}$ without making any MVA. The results were similar, but with greater uncertainties. Finally we note that the time shifts are not consistent with the structures moving along $\boldsymbol{B}$, since a projection of the satellite orbits onto a plane containing $\boldsymbol{B}$ (not shown here) indicates that the satellites would encounter the structures in a different order (to wit: 4, 2, 1, 3 or the reverse of that).

To test the assumption that these structures are elongated, we note that the orientation of the structure in interval (1) is such that satellites 1 and 4 cross the structure almost simultaneously, but at different positions along the structure. The fact that the signals observed by both satellites look very similar indicates that there is little variation along the structure on scales comparable to the satellite separation. The same is true for satellites 2 and 3. The slight difference in the structures observed by satellites 1 and 4 compared to those observed by satellites 2 and 3 can be interpreted as a slow temporal evolution.

Having made it probable that the structures are elongated sheets, it is natural to interpret them as quasi-static electric field structures, associated with sheets of up- and downgoing Birkeland currents. To test this interpretation, we consider the angles calculated in MVA on the electric and magnetic field data in both intervals. Since the magnetic field perturbations are parallel to an infinitely long current sheet, and the electric field perpendicular to it, in the absence of any background electric field, we can thus obtain an independent estimate of the orientation of the structures. The results are shown in columns three and four of Table 2, and it can be seen that the results from the MVA of $d\boldsymbol{B}$ are consistent with the orientations derived from the cross-correlation analyses. For interval (1) the result from the MVA of $\boldsymbol{E}$ is reasonably consistent, whereas for interval (3) it is considerably different. The fact that the rotation of the electric field from a normal direction to the current sheet is clockwise is consistent with this rotation being associated with an induced electric field due to the rapid motion of the structure. Due to the large uncertainties in the angles, it is difficult to make a quantitative check of this, but this explanation is consistent with the much less pronounced rotation of the electric field of interval (1).

Using the orientations and velocities of the structures determined above, we note that the widths of the electric field structures in intervals (1) and (3) are approximately 140 km and 120 km, respectively, defining the width as twice the width at half maximum. Mapping down to the ionosphere reduces these values by a factor of around 10.

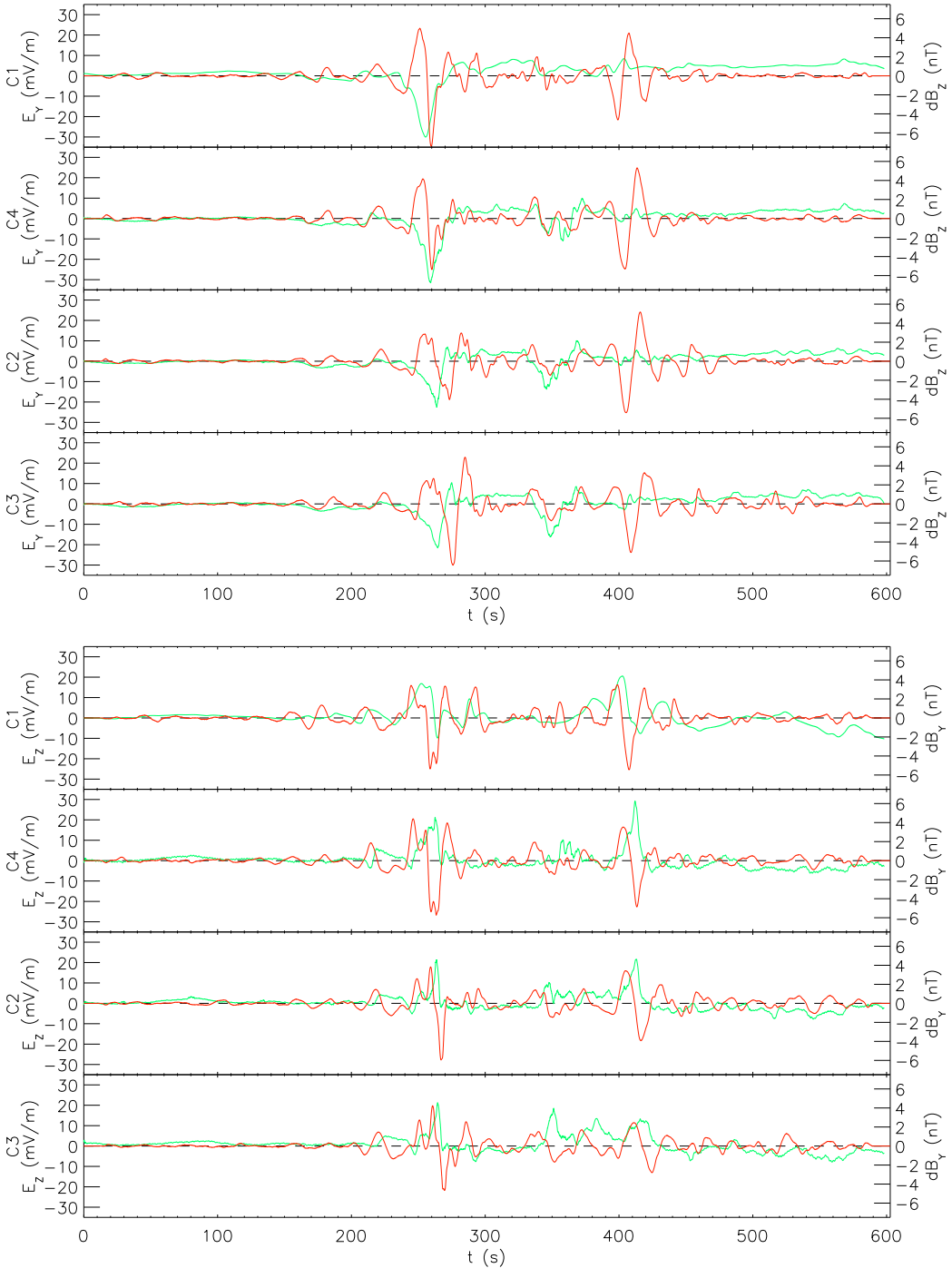

Fig. 4. Comparison of mutually perpendicular components of the electric field $\boldsymbol{E}$ (green) and the residual magnetic field $d\boldsymbol{B}$ (red) for the four Cluster satellites. y and z are approximately to the geomagnetic west and north, respectively, and the order of the panels is the order in which the Cluster satellites encounter the quasi-static structures of intervals (1) and (3).

From the above, it seems likely that the electric and magnetic field variations observed in interval (1) and (3) are elongated, quasi-static electric field structures associated with sheets of Birkeland currents, moving perpendicular to the background magnetic field, whereas the variations in interval (2) seem to be temporal variations. We will now try to further verify this hypothesis by studying the detailed relation between $\boldsymbol{E}$ and $d\boldsymbol{B}$.

In Fig. 4 the first four panels show the y component of the electric field E_y (corresponding roughly to geomagnetic "west"), and the perpendicular magnetic field component dB_z ("north"). The data from each satellite are shown in the order in which they encounter the quasi-static structures of intervals (1) and (3). The next four panels show E_z and dB_y.

We first draw attention to interval (2), where there appears to exist a region of quasi-periodic variations with a clear correlation between E_y and dB_z, between approximately t=330 s and 380 s for satellites 4, 2, and 3. For satellite 1 this is less clear, and the signals are generally weaker, especially for the electric field. We point out again that the electric field of satellite 1 is only determined at spin resolution, and has to be interpreted with a certain amount of wariness. Inspection of the data shows that the period of the variations is of the order of 20–40 s. For E_z and dB_y there is a corresponding anticorrelation. (Although less clear, in particular there seems to be superposed an increasing unipolar electric field from approximately t=350 s to 400 s.) The correlation of E_y and dB_z, the anticorrelation of E_z and dB_z, and the absence of any appreciable phase shift is consistent with a downward travelling Alfvén wave. To check this interpretation, we estimate the E/B ratio for these variations and obtaint approximately E/B=4400 km/s±1200 km/s. This should be compared to the actual Alfvén velocity v_A. We can estimate this from measurements of particle densities. In order to verify the measurements we have compared ion data from the Cluster Ion Spectrometry (CIS) instrument (Rème et al., 2001), electron data from the PEACE instrument and the electron density determined from the plasma frequency measured by the Waves of High Frequency and Sounder for Probing of Electron Density by Relaxation (WHISPER) instrument (Trotignon et al., 2003). All these instruments show similar values of the electron density n_e within interval (2); n_e varies between 0.2 and 0.8 cm^{-3}. (We have not used the electron density measurements based on the spacecraft potential, since these are problematic at such low densities.) Assuming a plasma containing of an equal mixture of oxygen and hydrogen ions (which is consistent with the CIS data), and using the average value of 406 nT for the total magnetic field, we obtain an Alfvén velocity between 3400 and 6800 km/s. One can also take the CIS measurements at face value, and calculate an average of v_A over all measurement points of satellites 1, 3, and 4 (the CIS instrument on satellite 2 was not operating correctly during this time). This yields v_A=7170 km/s±4220 km/s, where the uncertainty represents one standard deviation and the average is based on 90 data points. The large uncertainty is mainly due to variations in the ratio between the density of Hydrogen and Oxygen ions. Although the uncertainties are large, the E/B ratio can thus be considered to be consistent with the ambient Alfvén velocity.

Furthermore, PEACE data presented in the companion paper, show bi-directional electron beams of energies of around 50–100 eV for this time interval, most clearly in measurements from satellites 3 and 4. Such bidirectional beams can be produced by acceleration of Alfvén waves which have a parallel electric field in the inertial or kinetic limit (Stasiewicz et al., 2000). We also note that the local hydrogen and oxygen ion cyclotron frequencies are Ω_{C,H^+}=8 Hz and Ω_{C,O^+}=2 Hz, so that the frequencies of the observed oscillations are well below the ion cyclotron frequency, as they should be for Alfvén waves.

The wave signatures measured by satellites 4, 2 and 3 look rather similar to each other, but not to those of satellite 1. Even though we consider the usual caveat for the time resolution of the electric field measurements from satellite 1, this seems to be also true for the magnetic field fluctuations which are not affected by the difference in sampling frequency. If these differences are associated with the perpendicular wavelength $\lambda_\perp$ of the Alfvén waves (note that for any inertial or kinetic Alfvén wave the value of the parallel electric field is related to the perpendicular gradient of $\boldsymbol{E}$, and the wave must thus have a perpendicular variation), we can conclude that such a $\lambda_\perp$ should be larger than the separation between satellite 1 and any of the other satellites, projected on the perpendicular wave vector $\boldsymbol{k}_\perp$. Assuming the $\boldsymbol{k}_\perp$ to be perpendicular to the direction of minimum variance of $d\boldsymbol{B}$ in interval (2), we obtain a lower limit of $\lambda_\perp$ to be around 120 km. An upper limit cannot really be obtained, but the appreciable difference in the signal between satellite 1 and the other satellites makes it probable that $\lambda_\perp$ is not greater than 120 km by more than an order of magnitude. A question is if the waves are planar; here it is difficult to say, since the perpendicular wavelength is of the same order as the satellite separations. Future work with similar events with different types of satellite separations needs to be done to answer this question.

(We pause here to note that this estimate of $\lambda_\perp$ allows us to verify that the assumption that $\boldsymbol{E}\cdot\boldsymbol{B}$=0 does not introduce any large errors for the calculated third component of $\boldsymbol{E}$, even for the Alfvénic electric fields of region (2). Using the parameters above and an electron temperature of T_e=2.5 keV, which is typical for the plasma sheet boundary layer, we note that the plasma β is greater than m_e/m_i. We are then in the regime of kinetic Alfvén waves, and the ratio of $E_\parallel$ to $E_\perp$ is given by $\left|\frac{E_\parallel}{E_\perp}\right| = \frac{k_\parallel k_\perp \rho_s^2}{1+k_\perp^2\rho_i^2}$, where ρ_s is the ion radius at electron temperature, ρ_i is the ion thermal gyro radius, and $k_\parallel$ and $k_\perp$ are the parallel and perpendicular wave numbers (Stasiewicz et al., 2000). Estimating $k_\parallel$ from the value of the Alfvén velocity above and a frequency of ∼0.1 Hz, and using T_i=2T_e, we obtain $\left|\frac{E_\parallel}{E_\perp}\right|$=2%. Thus, we do not introduce any large errors when calculating the third component from $\boldsymbol{E}\cdot\boldsymbol{B}$=0.)

For the intense electric field structures of intervals (1) and (3), however, there is no correlation between electric and magnetic fields. Instead the large electric fields can be seen to coincide with the largest positive gradients of $d\boldsymbol{B}$. Taking the geometry of the sheets into account, and invoking the above interpretation of the quasi-static nature of the magnetic field structures, we interpret these gradients as sheets of downward directed current. We thus find that the large electric fields of intervals (1) and (3) are high-altitude analogues to the large diverging electric fields found in the downward current region at Freja and FAST altitudes of a few thousand kilometers, often being associated with upward electron beams of energies from a few 100 eV to over a keV (Marklund et al., 1997; Carlson et al., 1998), although the structures here observed are unipolar. Also, the event studied by Marklund et al. (2001) was associated with an downward

current, and an energetic upward electron beam. If these fields really are of a similar nature, we should expect to also observe upward electron beams for these events, and indeed PEACE data (presented in the companion paper) show upward electron beams collocated with the intense electric field structures. The details of these electron beams and their association with the electric field structures are discussed in the companion paper.

Finally, we point out that Figs. 2, 3, and 4 suggest that there is a rather constant background electric field from around t=280 s and onwards, i.e. behind the "front" of the leading one of the moving structures. Closer inspection shows this field to be about 4 mV/m and directed to the geomagnetic southwest. This is consistent with the normally southwardly directed convection electric field associated with the Southern Hemisphere, negative morning cell of the usual two-cell pattern associated with southward IMF conditions.

4 Discussion

The results of Sect. 3 show that we can use the multipoint measurements to separate between spatial and temporal variation. We thus interpret the above results as two quasi-static electric field structures associated with elongated current sheets, moving in a generally southward direction, and sandwiching a region of downward travelling Alfvénic waves. The fact that they are travelling southwards (i.e. polewards) may indicate that they are a part of the general expansion of the poleward part of the auroral oval. That these structures are located at the poleward boundary of the oval is clear from the particle data, which identify the region studied here as a part of the plasma sheet boundary layer. The different deviation from southward motion of the two structures may be related to meso-scale variations in this global southward motion.

The fact that the perpendicular components of $\boldsymbol{E}$ and $d\boldsymbol{B}$ are not correlated to each other within the regions of the intense quasi-static electric fields, indicates that the ionospheric conductivity below them is not constant, since that would result in a correlation. Instead, the intense electric fields are likely to be set up, in order to maintain current closure through regions of low conductivity. We can still estimate this conductivity by calculating the ratio between the magnitudes of perpendicular components of $d\boldsymbol{B}$ and $\boldsymbol{E}$, since for an extended current sheet

$$\Sigma_P = \frac{J_P}{E_n} = \frac{\int j_{\parallel}\, dx}{E_n} = \frac{\int \frac{\partial B_t}{\partial n} dn}{\mu_0 E_n} = \frac{B_t}{\mu_0 E_n}, \quad (1)$$

where t represents the coordinate tangential to the sheet, n the coordinate normal to the sheet, Σ_P is the Pedersen conductivity, J_p the Pedersen current, and $j_{//}$ the downward Birkeland current. The fields are to be evaluated at the ionospheric level. Assuming no potential drop between the Cluster altitude and the ionosphere we can instead evaluate the ratio between the fields at the Cluster altitude, which yields an approximate value of Σ_P=0.1 S. However, since the integrated potential of the electric field shows a good correlation with the energies of upward accelerated electrons, it is probable that the electric field does not map unattenuated down to the ionosphere. Thus, it is probable that the conductivity is larger than this, but probably not more than by an order of magnitude. It is thus comparable to the value of around 1 S, which is the approximate value given in earlier studies of the return current region (Karlsson and Marklund, 1996).

The low ionospheric conductivity of the downward current region is likely due to an outflow of the ionospheric electrons carrying the current. Numerical calculations by Karlsson and Marklund (1998) show that currents of the order of $10\,\mu\mathrm{A/m}^2$ can evacuate the E-layer on time scales of seconds, and further evacuate large parts of the F-layer on time scales of a minute. The structures of intervals (1) and (3) both have a scale size of around 10 km at the ionospheric level. Moving at about 1 km/s the current system of the structures has around ten seconds in which to modify the fresh ionospheric plasma before it has passed it. This is enough to evacuate the E-region plasma and lower the height-integrated conductivity to the low values of around 1 S observed.

The whole configuration of large electric fields in downward current regions, associated with upward-going electron beams is very similar to the low-altitude observations of the downward current regions by Freja and FAST (Marklund et al., 1997; Carlson et al., 1998), and offers further proof that these electric field structures extend up to altitudes of $4\,R_E$. (The first multi-point measurement of such a quasi-static electric field in the downward current region was presented by Marklund et al., 2001.) We note that these findings are not consistent with the interpretation of observations by the Polar satellite from similar altitudes, that large electric fields at these altitudes are predominantly associated with Alfvénic fluctuations.

A difference between the quasi-static electric field structures observed here and the one observed by Marklund et al. (2001), and between many events observed by Freja, is that the structures described in this paper are unipolar, and not bipolar. However, it is difficult to determine the importance of this without studying more events. Probably potential structures in the downward current region can be S-shaped, as well as U-shaped, just as the auroral acceleration potential structures of the upward current regions.

One question worth asking is, however, why no sign is seen of any large perpendicular converging electric fields in upward current regions, mentioned above. This question is addressed in the companion paper. We only note here that the search for such structures have been reported to be unsuccessful using Polar data (Janhunen et al., 1999).

Turning to the downward traveling Alfvén waves of interval (2) we note that an obvious property of these is that they propagate in a region delimited by the two current sheets. It is possible that this region acts as a wave guide, due to gradients either produced by the currents or being associated with them in some other way (Leonovich et al., 1983). PEACE data shown in the companion paper show that the borders

between regions (1), (2) and (3) are really associated with gradients in particle fluxes. We also note that the estimated perpendicular wavelength $\lambda_\perp$ is of the same order of magnitude as the width of the region where the Alfvén waves propagate, which is consistent with these waves being a fundamental wave-guide mode (Wright, 1994; Griffiths, 1999). Further studies are needed to verify if this is a common configuration at these altitudes.

Another question is how these waves are excited. The periods of the observed waves are interesting, since they are greater than those associated with standing Alfvén waves in the ionospheric Alfvén resonator ($T\sim$1 s), but shorter than periods associated with the Pi2 pulsations associated with substorm onset ($T\sim$40–150 s) or field line resonances ($T\sim$100–1000 s), although they could be harmonics of these. Recently fluctuations with shorter periods than those of Pi2 have been observed in the magnetotail in association with substorm onset, but these are not likely to be Alfvénic and furthermore have periods shorter than 10 s (Sigsbee et al., 2002). Another possibility is that they are Alfvén waves excited by the large field-aligned currents surrounding the "wave guide" region and propagated into it. Further work is needed to estimate the frequencies resulting from a geometry applicable to the measurements presented here, but we note that the growth rate of kinetic Alfvén waves generated by an electron beam maximizes for a perpendicular wavelength of $\lambda_\perp = \frac{\rho_i}{2\pi}$, where $\rho_i = \frac{m_i v_\perp}{eB}$ is the ion gyro radius, m_i the ion mass, $v_\perp$ the perpendicular thermal velocity and e the elementary charge (Hasegawa, 1979). For an oxygen plasma with a temperature of 5 keV, which is typical for the plasma sheet boundary layer, we get $\lambda_\perp\sim$300 km which is in good agreement with the estimate given from the measurements above.

5 Conclusions

We have shown how Cluster multi-point measurements can resolve the spatio-temporal ambiguities on auroral field lines. The event studied here contains two regions where the variations in the electric and magnetic fields are seen to be mainly quasi-static, and a region between these, where the variations are mainly temporal. We believe this to be a unique high-resolution and detailed separation of the spatial and temporal variations of the fields associated with the high-altitude region above the auroral acceleration region.

The fact that the intense quasi-static electric fields structures are seen in the downward current region, and are associated with upward accelerated electrons and low ionospheric conductivities show that they are high-altitude analogues to the intense return-current electric field structures observed by Freja and FAST. They are seen to be stable (although evolving slightly) on a time scale of around half a minute.

The signatures of the temporal variations are consistent with downward travelling Alfvén waves, with a period of 20–40 s. This is a period somewhere between those expected from either field line resonances, or resonances within the ionospheric Alfvén resonator (which anyway is located below the observations). The origin of these waves is an open question and needs to be addressed in later studies. The multipoint measurements enables us to determine a lower limit of the perpendicular scale-size $\lambda_\perp$ of these waves. The fact that $\lambda_\perp > 120$ km might indicate that it is of approximately of the same size as the perpendicular (to $\boldsymbol{B}$) distance between the quasi-static structures. This, in turn, might suggest that the Alfvén waves are ducted between these, in a fundamental wave guide mode.

The fact that the largest electric fields are associated with the quasi-static structures suggests that the electromagnetic energy transport associated with these structures dominate over that of the Alfvén waves. This issue is further addressed in the companion paper, and will also be the subject of future work.

Acknowledgements. We are grateful to A. Fazakerly for providing PEACE data and to H. Nilsson for providing CIS data. We thank A. de Assis and N. Brenning for useful and entertaining discussions. One of the authors (S. Figueiredo) acknowledges the support from the Fundação para a Ciência e a Tecnologia (FCT) under the grant SFRH/BD/6211/2001.

Topical Editor T. Pulkkinen thanks M. Mogilevsky and another referee for their help in evaluating this paper.

References

Balogh, A., Dunlop, M. W., Cowley, S. W. H., Southwood, D. J., Thomlinson, J. G., Glassmeier, K. H., Musmann, G., Luhr, H., Buchert, S., Acuna, M. H., Fairfield, D. H., Slavin, J. A., Riedler, W., Schwingenschuh, K., and Kivelson, M. G.: The Cluster magnetic field investigation, Space Sci. Rev., 79, 65–92, 1997.

Carlson, C. W., McFadden, J. P., Ergun, R. E., Temerin, M., Peria, W., Mozer, F. S., Klumpar, D. M., Shelley, E. G., Peterson, W. K., Möbius, E., Elphic, R., Strangeway, R., Cattell, C. A., and Pfaff, R.: FAST observations in the downward auroral current region: Energetic upgoing electron beams, parallel potential drops, and ion heating, Geophys. Res. Lett., 25, 2017–2020, 1998.

Dunlop, M. W., Balogh, A., and Glassmeier, K.-H.: Four-point Cluster application of magnetic field analysis tool: The discontinuity analyzer, J. Geophys. Res., 107, 1385, 2002.

Griffiths, D. J.: Introduction to Electrodynamics, IIIrd edition, Prentice Hall, 1999.

Gustafsson, G., André, M., Carozzi, T., Eriksson, A. I., Fälthammar, C.-G., Grard, R., Holmgren, G., Holtet, J. A., Ivchenko, N., Karlsson, T., Khotyaintsev, Y., Klimov, S., Laakso, H., Lindqvist, P.-A., Lybekk, B., Marklund, G., Mozer, F., Mursula, K., Pedersen, A., Popielawska, B., Savin, S., Stasiewicz, K., Tanskanen, P., Vaivads, A., and Wahlund, J.-E.: First results of electric field and density observations by Cluster EFW based on initial months of operation, Ann. Geophys., 19, 1219, 2001.

Gustafsson, G., Bostrom, R., Holback, B., Holmgren, G., Lundgren, A., Stasiewicz, K., Åhlen, L., Mozer, F. S., Pankow, D., Harvey, P., Berg, P., Ulrich, R., Pedersen, A., Schmidt, R., Butler, A., Fransen, A. W. C., Klinge, D., Thomsen, M., Fälthammar, C.-G., Lindqvist, P.-A., Christenson, S., Holtet, J., Lybekk, B., Sten, T. A., Tanskanen, P., Lappalainen, K., and Wygant, J.: The electric field and wave experiment for the Cluster mission, Space Sci. Rev., 79, 137–156, 1997.

Hasegawa, A.: Excitation of Alfvén Waves by Bouncing Electron Beams – An Origin of Nightside Magnetic Pulsations, Geophys. Res. Lett., 6, 664, 1979.

Ivchenko, N., Marklund, G., Lynch, K., Pietrowski, D., Torbert, R., Primdahl, F., and Ranta, A.: Quasiperiodic oscillations observed at the edge of an auroral arc by Auroral Turbulence 2, Geophys. Res. Lett., 26, 3365, 1999.

Janhunen, P., Olsson, A., Mozer, F. S., and Laakso, H.: How does the U-shaped potential close above the acceleration region? A study using Polar data, Ann. Geophys., 17, 1276–1283, 1999.

Johansson, T., Figueiredo, S., Karlsson, T., Marklund, G. T., Fazakerley, A., Buchert, S., Lindqvist, P.-A., and Nilsson, H.: Intense High-Altitude Electric Fields – Temporal and Spatial Characteristics, 22, 7, 2485–2495, 2004.

Johnstone, A. D., Alsop, C., Burge, S., Carter, P. J., Coates, A. J., Coker, A. J., Fazakerley, A. N., Grande, M., Gowen, R. A., Gurgiolo, C., Hancock, B. K., Narheim, B., Preece, A., Sheather, P. H., Winningham, J. D., and Woodliffe, R. D.: Peace: A Plasma Electron and Current Experiment, Space Sci. Rev. 79, 351–398, 1997.

Jorgensen, A. M. and Spence, H. E.: On separating space and time variations of auroral precipitation: dual DMSP-F6 and -F8 observations, Adv. Space. Res., Vol. 20, Issue 3, 453, 1997.

Karlsson, T. and Marklund, G. T.: A statistical study of intense low-altitude auroral electric fields observed by Freja, Geophys. Res. Lett., 23, 1005, 1996.

Karlsson, T. and Marklund, G. T.: Simulations of Small-Scale Auroral Current Closure in the Return Current Region, in Physics of Space Plasmas, No. 15, Proc. of the 1998 Cambridge Symposium/Workshop in Geoplasma Physics on "Multiscale Phenomena in Space Plasmas II", Cascais, Portugal, 1998, edited by Chang, T. and Jasperse, J. R., MIT Center for Theoretical Geo/Cosmo Plasma Physics, Cambridge, Massachusetts, 401–406, 1998.

Leonovich, A. S., Mazur, V. A., and Senatorov, V. N.: Alfvén Waveguide, Sov. Phys., JETP, 58, (1), 83–85, 1983.

Lynch, K. A., Pietrowski, D., Ivchenko, N., Marklund, G., Torbert, R., and Primdahl, F.: Multi-point electron measurements in a nightside auroral arc: Auroral Turbulence II particle observations, Geophys. Res. Lett., 26, 3361, 1999.

Marklund, G. T., Ivchenko, N., Karlsson, T., Fazakerley, A., Dunlop, M., Lindqvist, P.-A., Buchert, S., Owen, C., Taylor, M., Vaivads, A., Carter, P., André, M., and Balogh, A.: Temporal evolution of the electric field accelerating electrons away from the auroral ionosphere, Nature, 414, 724, 2001.

Marklund, G. T. and Karlsson, T.: Characteristics of the Auroral Particle Acceleration in the Upward and Downward Current Regions, Phys. Chem. of the Earth C, 26, 81–96, 2001.

Marklund, G., Karlsson, T., and Clemmons, J.: On Low-Altitude Particle Acceleration and Intense Electric Fields and their Relationship to Black Aurora, J. Geophys. Res., 102, 17 509–17 522, 1997.

Pedersen, A., Decreau, P., Escoubet, C.-P., Gustafsson, G., Laakso, H., Lindqvist, P.-A., Lybekk, B., Masson, A., Mozer, F., and Vaivads, A.: Four-point high time resolution information on electron densities by the electric field experiments (EFW) on Cluster, Ann. Geophys., 19, 1483–1489, 2001.

Rème, H., Aoustin, H., Bosqued, J., et al.: First multispacecraft ion measurements in and near the Earth's magnetosphere with the identical Cluster ion spectrometry (CIS) instrument, Ann. Geophys., 19, 10–12, 1303–1354, 2001.

Sigsbee, K., Cattell, C. A., Fairfield, D., Tsuruda, K., and Kokobun, S.: Geotail observations of low-frequency waves and high-speed earthward flows during substorm onset in the near magnetotail from 10 to 13 R_E, J. Geophys. Res, 107, (A7), SMP 27, doi:10.1029/2001JA000166, 2002.

Stasiewicz, K., Bellan, P., Chaston, C., Lysak, R., Maggs, J., Pokhotelov, O., Seyler, C., Shukla, P., Stenflo, L., Streltsov, A., and Wahlund, J.-E.: Small Scale Alfvénic Structure in the Aurora, Space Science Reviews, 92, 423–533, 2000.

Trotignon, J. G., Rauch, J. L., Décréu, P. M. E., Canu, P., and Lemaire, J.: Active and passive plasma wave investigations in the earth's environment: The Cluster/Whisper experiment, Adv. Space Res., 31, 5, 1449–1454, 2003.

Weimer, D. W. and Gurnett, D. A.: Large-amplitude auroral electric fields measured with DE 1, J. Geophys. Res., 98, 13 557–13 564, 1993.

Wright, A. N.: Dispersion and wave coupling in inhomogeneous MHD waveguides, J. Geophys. Res., 99, 159–167, 1994.